Journal of Hazardous Materials 166 (2009) 788–795

Contents lists available at ScienceDirect

Journal of Hazardous Materials

journal homepage: www.elsevier.com/locate/jhazmat

Removal of oxyanions from synthetic wastewater via carbonation process of calcium hydroxide: Applied and fundamental aspects

G. Montes-Hernandez[a,b,*], N. Concha-Lozano[a], F. Renard[a,c], E. Quirico[b]

[a] LGCA, University Joseph Fourier, Observatoire des Sciences de l'Univers de Grenoble and CNRS, BP 53 X, 38042 Grenoble Cedex 9, France
[b] LPG, University Joseph Fourier, Observatoire des Sciences de l'Univers de Grenoble and CNRS, BP 53 X, 38042 Grenoble Cedex 9, France
[c] Physics of Geological Processes, University of Oslo, Norway

ARTICLE INFO

Article history:
Received 28 July 2008
Received in revised form 7 October 2008
Accepted 25 November 2008
Available online 6 December 2008

Keywords:
Oxyanions
Aqueous carbonation
Calcium hydroxide
Water treatment
Mineralization of CO_2

ABSTRACT

Removal of oxyanions (selenite, selenate, arsenate, phosphate and nitrate) during calcite formation was experimentally studied using aqueous carbonation of calcium hydroxide under moderate pressure ($P_{CO2} \cong 20$ bar) and temperature (30 °C). The effects of $Ca(OH)_2$ dose (10 and 20 g), $Ca(OH)_2$ source (commercial pure material or alkaline paper mill waste) and oxyanion initial concentration (from 0 to 70 mg atom/L) were investigated for this anisobaric gas–liquid–solid system.

The $Ca(OH)_2$ carbonation reaction allowed successfully the removal of selenite (>90%), arsenate (>78%) and phosphate (≅100%) from synthetic solutions. Conversely, nitrate and selenate had not any physicochemical affinity/effect during calcite formation.

The rate of CO_2 transfer during calcite formation in presence of oxyanions was equal or slower than for an oxyanion-free system, allowing to define a retarding kinetic factor *RF* that can vary between 0 (no retarding effect) to 1 (total inhibition). For selenite and phosphate *RF* was quite high, close to 0.3. A small retarding effect was detected for arsenate ($RF \approx 0.05$) and no retarding effect was detected for selenate and nitrate ($RF \approx 0$). In general, *RF* depends on the oxyanion initial concentration, oxyanion nature and $Ca(OH)_2$ dose.

The presence of oxyanions could also influence the crystal morphology and aggregation/agglomeration process. For example, a *c*-axis elongation of calcite crystals was clearly observed at the equilibrium, for calcite formation in presence of selenite and phosphate.

The oxyanions removal process proposed herein was inspired on the common physicochemical treatment of wastewater using calcium hydroxide ($Ca(OH)_2$). The particularity, for this novel method is the simultaneous calcium hydroxide carbonation with compressed carbon dioxide in order to stabilise the solid matter. This economical and ecological method could allow the removal of various oxyanions as well as the ex situ mineral sequestration of CO_2; particularly, when the $Ca(OH)_2$ source comes from alkaline solid waste.

1. Introduction

Anions are typically mobile in soils and groundwater since most natural minerals have net negative surface charges. A number of anions, particularly inorganic oxyanions such as nitrate, chromate, arsenate, molybdate, selenite and selenate, can be toxic to humans or wildlife at μg/L to mg/L concentrations. Others such as phosphates or nitrates can perturb the natural environments enhancing the eutrophication processes. Removal of oxyanions from water has been achieved by coprecipitation [1,2], reverse osmometry [3], chemical reduction to less soluble species [4], and adsorbing colloid flotation (ACF) methods [5,6]. These methods generally need large and complicated facilities due to various equipment and reagents used in a series of treatments. In addition, the removal of toxic oxyanions is much more difficult than that of the cations because anions with a similar structure, such as nitrate, sulphate and phosphate often coexist in nature with high concentrations. Although the adsorptive removal of the toxic oxyanions from solution using conventional adsorbents, such as activated carbon [7,8], tanning gel [9], zeolites [10], iron oxides [11–14], and aluminium oxide [15], have been reported, they are not selective and sometimes with low effectiveness. Searching effective adsorbents, reagents and/or novel methods for the removal of the oxyanions represents an important environmental remediation issue.

The formation of solid carbonates from aqueous solutions or slurries containing divalent cations and carbon dioxide (CO_2) is a complex process of considerable importance in the ecological,

* Corresponding author.
E-mail addresses: German.MONTES-HERNANDEZ@obs.ujf-grenoble.fr, german_montes@hotmail.com (G. Montes-Hernandez).

0304-3894/$ – see front matter © 2009 Elsevier B.V. All rights reserved.
doi:10.1016/j.jhazmat.2008.11.120

geochemical, biological and industrial areas. This process could also be used for the removal of toxic oxyanions by incorporation and/or adsorption in/on solid structure. This was recently demonstrated using heterogeneous or homogeneous systems to incorporate oxyanions in calcite, i.e. the substitution of carbonate ion (CO_3^{-2}) by an oxyanion during calcite crystal precipitation/growth ([16–20] and others).

Recent studies carried out in our laboratory have shown that the aqueous carbonation of calcium hydroxide in contact with compressed CO_2 at moderate temperature allows the synthesis of fine particles of calcite [21,22]. There, it was demonstrated that the pressure, the temperature and the dissolved quantity of CO_2 have significant effect on the average particle size, specific surface area, initial rate of precipitation, and on the morphology of calcium carbonate crystals. In contrast, the PTx conditions used herein have not effect on the aqueous carbonation efficiency of $Ca(OH)_2$. The reaction mechanism of calcite precipitation via aqueous carbonation of $Ca(OH)_2$ was then described by the global reaction,

$$Ca(OH)_{2(s)} + CO_{2(aq)} \rightarrow CaCO_{3(s)} + H_2O \quad (1)$$

this is an exothermic process that concerns simultaneously the aqueous dissolution of $Ca(OH)_2$,

$$Ca(OH)_{2(s)} \xrightarrow{water} Ca^{2+} + 2OH^- \quad (2)$$

and the dissociation of aqueous CO_2 into water,

$$CO_{2(aq)} + H_2O \rightarrow {CO_3}^{2-} + 2H^+ \quad (3)$$

These processes produce a fast supersaturation (S_I) of solution with respect to calcite,

$$S_I = \frac{(Ca^{2+})({CO_3}^{2-})}{K_{sp}} > 1 \quad (4)$$

where (Ca^{2+}) and $({CO_3}^{2-})$ are the activities of calcium and carbonate ions in the solution, respectively, and K_{sp} is the thermodynamic solubility product of calcite. Then, the nucleation stage (formation of nuclei or critical cluster) takes place in the system,

$$Ca^{2+} + {CO_3}^{2-} \rightarrow CaCO_3(\text{nuclei}) \quad (5)$$

Finally, the crystal growth occurs spontaneously until the equilibrium calcite and the solution is reached,

$$CaCO_3(\text{nuclei}) \rightarrow CaCO_3(\text{calcite}) \quad (6)$$

The metastable crystalline phases of $CaCO_3$, such as vaterite and aragonite, were not identified in the X-ray diffraction spectra of the final products during the $Ca(OH)_2$ carbonation process under these experimental conditions [22].

In general, the polymorphism of crystalline calcium carbonate depends mainly on the precipitation conditions. Many experimental studies have focused on the precipitation of the various forms of calcium carbonate and the conditions under which these may be produced, including the initial supersaturation, temperature, pressure, pH and hydrodynamics [23]. The effect of impurities and additives has also been well studied [24–37]. However, the effects of dissolved oxyanions on the precipitation rate and on the morphology of calcite crystals are still poorly known and rarely reported in the literature.

The present study is focused on both applied and fundamental aspects. Firstly, the calcium hydroxide carbonation with compressed CO_2 was used in order to estimate a removal efficiency of oxyanions (selenite, selenate, arsenate, phosphate and nitrate) from a synthetic wastewater. Secondly, a simplified kinetic model was proposed to estimate the effects of these oxyanions on the rate of CO_2 transfer during calcite formation (retarding factor). The effects of oxyanions on the morphology and size of calcite crystal at the equilibrium state were also investigated.

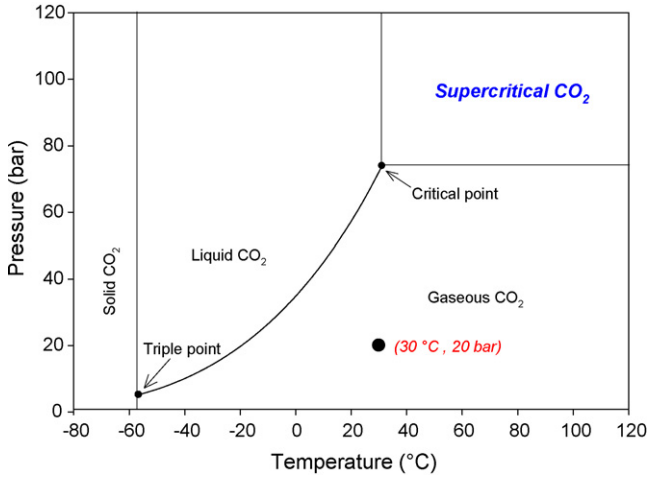

Fig. 1. Experimental *P–T* conditions represented on a pressure–temperature phase diagram for CO_2.

2. Materials and methods

2.1. $Ca(OH)_2$ aqueous carbonation with compressed CO_2

One litre of high-purity water with an electrical resistivity of 18.2 MΩ cm, 20 g of commercial portlandite $Ca(OH)_2$ (calcium hydroxide provided by Sigma–Aldrich) with 96% chemical purity (3% $CaCO_3$ and 1% other impurities) and three different quantities (from 0 to 250 mg) of sodium selenite pentahydrate $Na_2SeO_3{\cdot}5(H_2O)$, sodium selenate Na_2SeO_4, sodium acid arsenate heptahydrate $Na_2HAsO_4{\cdot}7(H_2O)$, monosodium phosphate NaH_2PO_4 or sodium nitrate $NaNO_3$ (provided by Sigma–Aldrich) were placed in a titanium reactor (Parr© autoclave with internal volume of 2 L).

The solid particles were immediately dispersed by mechanical stirring (400 rpm). The dispersion (solution charged with a specific oxyanion + $Ca(OH)_2$ particles in excess) was then slightly heated to 30 °C using an oven specifically adapted to the reactor. When the dispersion temperature was stabilised 20 bar of CO_2 with 99.995% chemical purity (provided by Linde Gas S.A.) was injected in the reactor. This initial pressure of CO_2 corresponds to the total initial pressure in the system. At these temperature and pressure conditions, the vapour phase consists mainly of CO_2 gas in ideal state (Fig. 1). After CO_2 injection, the pressure drop was followed visually on a manometer as a function of time until CO_2 pressure reached an equilibrium value in this anisobaric gas–liquid–solid system. The rate of CO_2 transfer in the dispersion during calcite formation is directly related to this pressure drop. For several experiments, a pressure transducer (Keller series 33X) connected to a PC computer was coupled to the reactor to obtain a better precision and a continuous acquisition data of pressure drop at 1 Hz frequency (Fig. 2).

The effects of $Ca(OH)_2$ dose (10 and 20 g) and $Ca(OH)_2$ source (commercial pure material and from alkaline paper mill waste) and initial CO_2 pressure (20 and 30 bar) were investigated also for calcite formation in presence of selenite (230 mg/kg_{water}). Selenite oxyanion was selected here because preliminary carbonation experiments revealed high removal effectiveness for this oxyanion during calcite formation. In addition, the rate of CO_2 transfer into the dispersion was significantly retarded in presence of selenite.

Concerning $Ca(OH)_2$ source, note that the alkaline paper mill waste herein used contains about 55 wt% of portlandite $Ca(OH)_2$, 33 wt% of calcite $CaCO_3$ and 12 wt% of hydroxyapatite $Ca_{10}(PO_4)_6(OH)_2$. A more complete characterization and the

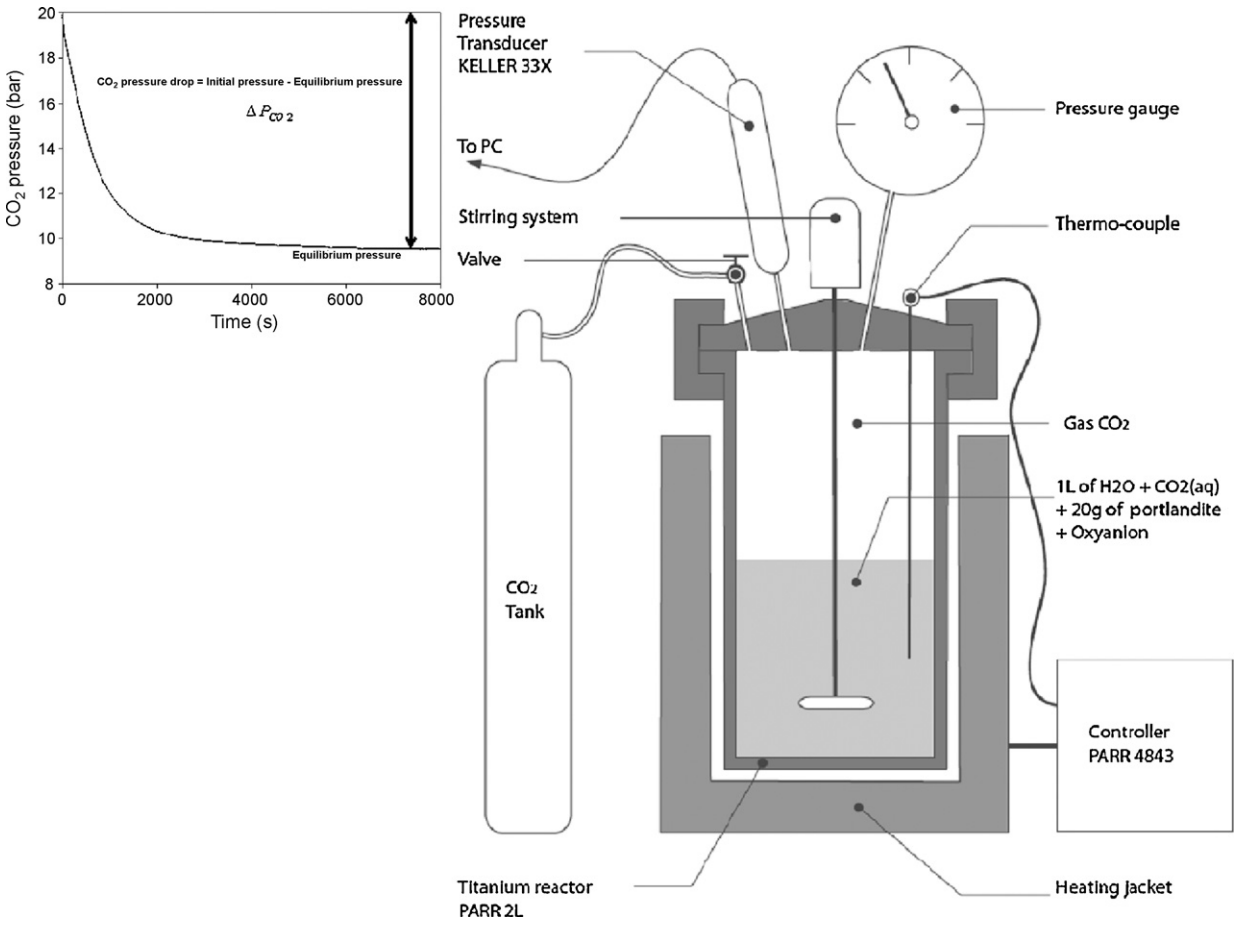

Fig. 2. Schematic experimental system for removal of oxyanions from synthetic wastewater via calcium hydroxide (portlandite) carbonation with compressed CO_2 in an anisobaric-stirred reactor. Inset: Continuous pressure evolution was monitored (one pressure value/s) using a pressure transducer linked to a PC computer. The pressure drop corresponds to the dissolution of CO_2 into solution, and the carbonation of portlandite.

carbonation process for this material have been described by Perez-Lopez et al. [38].

At the end of the experiment, the reaction cell was rapidly depressurized for about 5 min and the autoclave was disassembled. Immediately 20 ml of suspension were sampled and filtered in order to measure the pH and the oxyanion concentration. The solid product was recovered by centrifugation (30 min at 12,000 rpm) and decanting the supernatant solutions. Finally, the solid product was dried in the centrifugation flasks for 48 h at 65 °C, manually recovered and stored in plastic flasks.

2.2. Physicochemical characterization of aqueous solutions

The calcium, selenium and arsenic elements were dosed by Inductively Coupled Plasma Atomic Emission Spectrometry (ICP Perkin Elmer Optima 3300 DV). For this case, 10 ml of suspensions were filtered through a 0.22 μm pore-size filter and the obtained aqueous solutions were immediately acidified with a nitric acid solution and stored at 4 °C for further measurements. The PO_4^{3-} and NO_3^- ions were dosed by Ionic Chromatography (Dionex DX500). Here, 10 ml of suspensions were filtered through a 0.22 μm pore-size filter and the obtained aqueous solutions were stored at 4 °C for further measurements.

The pH was also systematically measured at the end of the experiment using a MA235 pH/ion analyser in filtered solutions (10 ml) without acidification. Note that the pH measurement was carried out at 25 °C after filtration, slight cooling and degasification of the solutions. While this measurement is not representative of in situ pH, it provides a reasonable estimate of the solution saturation index with respect to solid phases at standard conditions (25 °C and 1 atmosphere).

2.3. Morphological and chemical characterization of solid phase

Morphological analyses of six selected solid samples were performed by Scanning Electron Microscopy (SEM-FEG), using a Zeiss

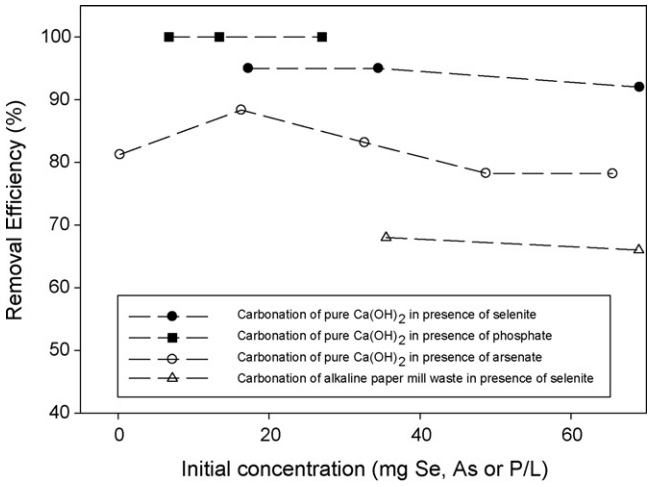

Fig. 3. Removal efficiency of selenite, arsenate and phosphate using $Ca(OH)_2$ carbonation with compressed CO_2. Note that the initial concentration (for a given oxyanion) must be superior to 0 mg/L in order to apply Eq. (7).

Ultra 55 microscope with a resolution around 1 nm at 15 kV. The samples (powders) were previously dispersed by ultrasound in absolute ethanol during five minutes. Then, one or two drops of suspension were deposited directly on the metallic supports for SEM observations. Isolated fine particles (oriented on carbon Ni grids) of the selected samples were also studied using a JEOL 3010 Transmission Electron Microscope (TEM) equipped with an energy dispersive X-ray analyzer (EDS) to image the morphology of the particles and to identify the elemental composition of the precipitates. Finally, the $Ca(OH)_2$ carbonation process was qualitatively controlled using infrared spectrometry, with a BRUKER HYPERION 3000 infrared microscope in transmission mode, with a MCT mono-detector at 2 and 4 cm^{-1} resolution. The typical size of the infrared spot onto the sample was ~25 μm × 25 μm. For these measurements, some aggregates of starting material and five solid products were manually compressed between two KBr windows in order to deposit a thin film of sample on a KBr window.

3. Results and discussion

3.1. Removal efficiency of oxyanions

The removal efficiency was calculated using a simple mass balance in the system,

$$\%\ \text{Removal} = \frac{C_0 - C_e}{C_0} \times 100 \quad (7)$$

where C_0 and C_e [mg atom/L] are the initial concentration of oxyanion and the concentration of oxyanion at the equilibrium, respectively.

The $Ca(OH)_2$ carbonation reaction using 20 g of commercial portlandite successfully removed selenite (>90%), arsenate (>78%) and phosphate (≈100%) from the synthetic solutions (Fig. 3). In general, at high dose of portlandite (>10 g), the removal efficiency was not influenced by the initial concentration for selenite, arsenate and phosphate. Conversely, the removal efficiency decreased significantly from 90 to 70% for selenite when a dose of 3 g of commercial portlandite was used.

For phosphate, a removal efficiency of 100% was calculated using Eq. (7) because this oxyanion was not detected in the solution using ionic chromatography (detection limit for phosphate = 0.6 mg/L). Various tests at atmospheric conditions revealed that the phosphate can be easily removed from a solution using portlandite $Ca(OH)_2$, possibly due to the formation of calcium phosphate compounds. This observation suggests that in our carbonation experiments, the phosphate removal from solution took place before carbonation process; and the pH decreased in the solution from 12.3 to 6.3 due to carbonation process had not any effect on the phosphate removal efficiency. On the other hand, in terms of removal efficiency, % removal of selenite decreased from 90 to 67% using 20 g of alkaline paper mill waste (Fig. 3), this possibly due to initial impurities content in this solid material (see [38]).

Finally, in our experiments, nitrate and selenate had insignificant physicochemical affinity during calcite formation (removal efficiency <5%).

3.2. Removal of selenite and arsenate at equilibrium

The removal of ions and molecules at solid-aqueous solution interfaces are important in numerous artificial and natural systems. In the last decades, several empirical, heuristic or mechanistic models (e.g. Langmuir, Freundlich, Redlich–Peterson, Brunauer–Emmett–Teller, and others) have been successfully used to fit and describe the removal processes, including adsorption, chemisorption, co-precipitation, incorporation, oxidation or photo-oxidation of ions and/or molecules at solid/aqueous solution interfaces. In general, the amount removed from solution at equilibrium q_e is correlated with the equilibrium concentration C_e. Herein, the removal isotherms ($q_e = f(C_e)$) for selenite and arsenate oxyanions were estimated as follows.

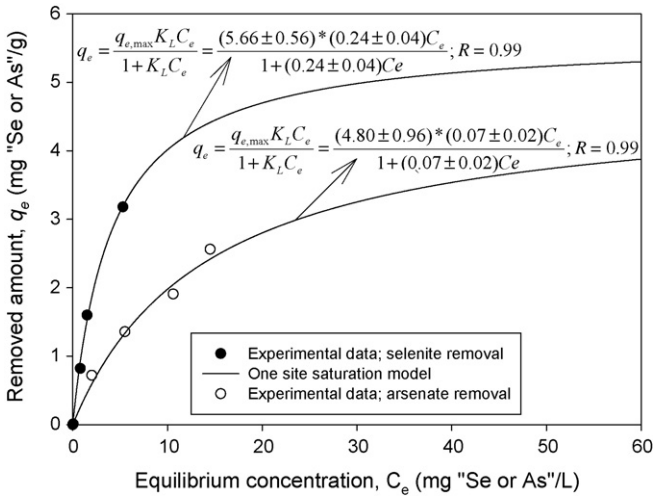

Fig. 4. Modelling of equilibrium isotherms for removal of selenite and arsenate from aqueous solutions using $Ca(OH)_2$ carbonation with compressed CO_2. The parameters $q_{e,max}$ and K_L were estimated using a nonlinear regression by least squares method. Herein the numerical errors for each parameter and correlation factor were reported.

The removed quantity of selenite or arsenate on/in calcite precipitates as a function of equilibrium concentration can be calculated using the following formula:

$$q_e = \frac{C_0 - C_e}{m} V \quad (8)$$

where C_0 represents the initial concentration of selenite or arsenate [mg Se or As/L]; C_e represents the concentration of selenite or arsenate at equilibrium [mg Se or As/L]; V represents the volume of the aqueous solution [L]; and m represents the mass of commercial portlandite $Ca(OH)_2$ [g]. The experimental data showed a saturation tendency of calcite sites for the studied concentration range. This removal behaviour can be easily modelled using a Langmuir approach. In the following paragraphs, we present a simple derivation of Langmuir equation, assuming one site saturation model. The differential form of this equation can be written as follows:

$$\frac{dq_e}{dC_e} = k_{qe}(q_{e,max} - q_e)^2 \quad (9)$$

where k_{qe} is a complex constant of removal process [g L/mg^2], $q_{e,max}$ is the maximal removed quantity of selenite or arsenate (site saturation state) [mg atom/g], q_e is the removed quantity of selenite or arsenate at equilibrium [mg atom/g] and C_e is the equilibrium concentration of solute [mg atom/L].

The integrated form of Eq. (9) for the boundary conditions $C_e = 0$ to $C_e = C_e$ and $q_e = 0$ to $q_e = q_e$ can be written as follows:

$$q_e = \frac{q_{e,max} C_e}{\frac{1}{k_{qe} q_{e,max}} + C_e} \quad (10)$$

where $(k_{qe})(q_{e,max}) = K_L$ can be interpreted as the equilibrium oxyanion-removal coefficient [L/mg]. Eq. (10) can be then rearranged to obtain the Langmuir equation:

$$q_e = \frac{q_{e,max} K_L C_e}{1 + K_L C_e} \quad (11)$$

Fitting our experimental data q_e vs. C_e by using Eq. (11) allows the estimation of $q_{e,max}$ and K_L. A nonlinear regression by least squares method was performed (see Fig. 4). Here, the $q_{e,max}$ value for arsenate (4.80 mg As/g) is slightly smaller than $q_{e,max}$ value for selenite

(5.66 mg Se/g), indicating that calcite precipitates have a better capacity to trap selenite during calcite formation. The numerical errors for each parameter and correlation factor for each isotherm were also reported in Fig. 4. Estimates of $q_{e,max}$ and K_L using Eq. (11) are fundamental to describe the removal process.

On the one hand, a liquid–solid distribution coefficient can be calculated as

$$K_D = K_L * q_{e,max} \quad (12)$$

where K_D [L/g or ml/g] is a physicochemical parameter widely used in geochemistry and/or in pollutant-mass transfer occurring in natural porous media. In addition, in engineering practice, this physicochemical parameter can be also associated to the thermodynamic parameters for the sorption/removal systems such as free energy (ΔG°), enthalpy (ΔH°) and entropy (ΔS°) in order to determine what processes will occur spontaneously. The liquid–solid distribution coefficient for selenite and arsenate are 1.35 and 0.34 L/g, respectively.

On the other hand, in technological applications, the equilibrium ion-removal coefficient K_L can be used to calculate a dimensionless separation factor or equilibrium parameter K_s, which is considered as a more reliable indicator of ion removal process (in fixed-bed or batch systems) [39]. This parameter is defined by the following relationship:

$$K_s = \frac{1}{1 + K_L C_0} \quad (13)$$

where K_s is a dimensionless separation factor, C_0 is the initial concentration of selenite or arsenate [mg Se or As/L] and K_L is the equilibrium oxyanion-removal coefficient [L/mg]. For favourable removal process, $0 < K_s < 1$; while $K_s > 1$ represents unfavourable removal process, and $K_s = 1$ indicates linear removal process. If $K_s = 0$ the removal process is irreversible. For the concentration range considered in this study, the removal process of selenite and arsenate ions is favourable (see Table 1).

Table 1
Separation factors for selenite and arsenate calculated by Eq. (13).

Selenite (K_L = 0.24 L/mg)			Arsenate (K_L = 0.07 L/mg)		
C_0 (mg Se/L)	K_s	Removal quality	C_0 (mg As/L)	K_s	Removal quality
17.25	0.19	Favourable	0.24	0.98	Favourable
34.50	0.11	Favourable	16.32	0.46	Favourable
69.1	0.06	Favourable	32.65	0.30	Favourable
			48.74	0.23	Favourable
			65.54	0.18	Favourable

Favourable removal process when $0 < K_s < 1$.

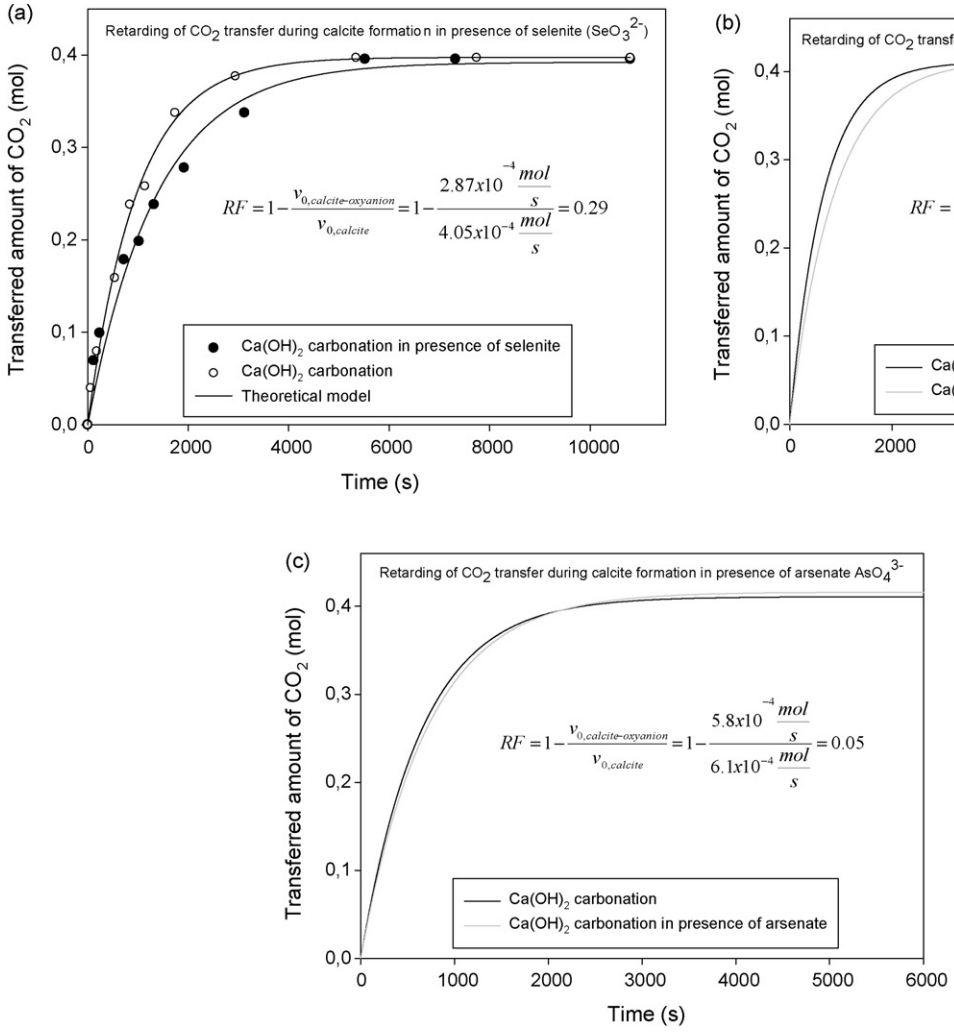

Fig. 5. Retarding effect of CO_2 transfer during calcite formation in presence of oxyanions. (a) selenite (69.1 mg Se/L); (b) phosphate (27.1 mg P/L) and (c) arsenate (48.7 mg As/L). *Operating conditions:* initial CO_2 pressure = 20 bar; reaction temperature = 30 °C; $Ca(OH)_2$ dose = 20 g; discontinuous visual acquisition of experimental data (pressure, time) for selenite and continuous automatic acquisition of experimental data (pressure value/s) for phosphate and arsenate. The parameters k_s and $n_{total.CO2,max}$ for exponential model were estimated by applying a nonlinear regression using the least-squares method.

3.3. Rate of CO_2 transfer into dispersion during calcite formation

It is well known that dissolved impurities can modify calcite crystal habits and induce crystallographic twining by sorption and/or incorporation of the impurities to the growing crystal surfaces, thereby, altering the growth kinetics. However, the effects of dissolved oxyanions on the calcite precipitation rate are rarely reported in the literature. In the current study, an indirect method was proposed to quantify the kinetic effects of oxyanions on the calcite precipitation/growth. For this case, the initial rate of CO_2 transfer during calcite formation in presence of a specific oxyanion was estimated. This rate was then compared with a reference rate, i.e. the initial rate of CO_2 transfer during calcite formation in the oxyanion-free system. Finally, a dimensionless retarding factor was calculated for each oxyanion. This method is described in the following paragraphs.

In a previous study, the CO_2 transfer in pure water and in a fly-ash–water suspension was satisfactory modelled using a kinetic pseudo-second-order model [20]. This model described a fast mass transfer step followed by a slow equilibration of mass transfer, this second step being frequently interpreted as a diffusion process. Several experiments on CO_2 transfer during calcite formation under P_{CO2} pressure in the range 10–40 bar initial pressure, have revealed that the kinetics of CO_2 transfer is controlled by the CO_2 absorption-dissociation process (Eq. (3)) and by calcite formation (Eqs. (5) and (6)).

The kinetics modelling of CO_2 transfer in our experiments can be successfully performed using a pseudo-first-order model according to the following expression:

$$\frac{dn_{total\_CO2,t}}{dt} = k_s(n_{total\_CO2,max} - n_{total\_CO2,t}) \quad (14)$$

where k_s is the rate constant of transferred CO_2 [1/s] for a given initial pressure of CO_2 in the system, $n_{total\_CO2,max}$ is the maximum transferred quantity of carbon dioxide at equilibrium [mol], $n_{total\_CO2,t}$ is the transferred quantity of carbon dioxide at any time, t, [mol]. The mol number of CO_2 $n_{total\_CO2,t}$ transferred into the suspension during calcite formation at any time, t, was calculated assuming ideal gas conditions as follows:

$$n_{total\_CO2,t} = \frac{(P_0 - P_t)V}{RT} \quad (15)$$

where P_0 represents the initial pressure of CO_2 (10 or 20 bar), P_t represents the monitored pressure of CO_2 at instant time t (bar), V is the reactor volume occupied with gas (1 L), T is the temperature of reaction (≈303 K) and R is the gas constant (0.08314472 L bar/K mol).

The integrated form of Eq. (14) for the boundary conditions $t = 0$ to $t = t$ and $n_{total\_CO2,t} = 0$ to $n_{total\_CO2,t} = n_{total\_CO2,t}$ is represented by a exponential equation:

$$n_{total\_CO2,t} = n_{total\_CO2,max}(1 - \exp(-k_s t)) \quad (16)$$

The parameters $n_{total\_CO2,max}$ and k_s can be used to calculate the initial rate of CO_2 transfer, $v_{0,s}$ [mol/s].

$$v_{0,s} = k_s * n_{total\_CO2,max} \quad (17)$$

Then, a dimensionless retarding factor (*RF*) can be expressed in terms of initial rate:

$$RF = 1 - \frac{v_{0,calcite-oxyanion}}{v_{0,calcite}} \quad (18)$$

where $v_{0,calcite\text{-}oxyanion}$ represents the initial rate of CO_2 transfer during calcite formation in presence of a given oxyanion [mol/s] and $v_{0,calcite}$ represents the initial reference rate of CO_2 transfer only during calcite formation [mol/s].

The parameters k_s and $n_{total\_CO2,max}$ were estimated by applying a nonlinear regression using the least-squares method. The numerical fit of the experimental-calculated kinetic curves at 20 bar and 30 °C ($n_{total\_CO2,t}$ vs. t) using Eq. (16) are shown in Fig. 5. The numerical calculations demonstrates that the initial rate of CO_2 transfer during calcite formation, was clearly retarded by dissolved selenium and phosphate ($0 < RF < 1$). A slight retarding effect was also detected for arsenate ($RF \approx 0.05$) (Fig. 5). In contrast, the rate of CO_2 transfer was not retarded by dissolved nitrate and selenate ($RF \approx 0$). This indirect method to measure the kinetic effects of oxyanions on the calcite precipitation demonstrates that the retarding factor depends on the oxyanion nature, oxyanion concentration and $Ca(OH)_2$ dose. In addition, the results globally confirm that sorption and/or incorporation of oxyanions to the growing crystal surfaces of calcite are the main causes of the retarding effect. This happens because non-reactive oxyanions such as selenate and nitrate (removal efficiency <5%, Eq. (7)) have not significant effect on the initial rate of CO_2 transfer during calcite formation. The EXAFS and XANES spectroscopy measurements and complementary adsorption experiments (pure calcite + dissolved oxyanion) are envisaged in the future to elucidate whether trapping of oxyanions is related to incorporation or to sorption mechanisms.

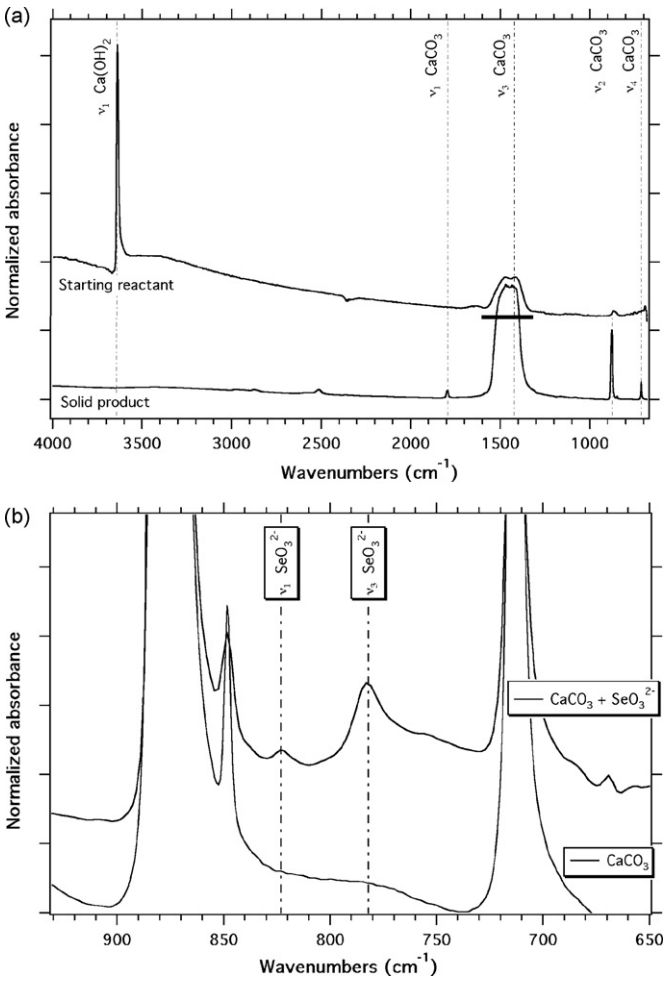

Fig. 6. (a) Infrared spectra of starting material ($Ca(OH)_2$ + residual carbonates) (top) and solid product as pure calcite (bottom). Note the strong ν_3 band of $CaCO_3$ is saturated (thick horizontal line). (b) Qualitative comparison of the infrared spectra of pure calcite and calcite doped with selenite. Note the spectral resolution was not the same in both spectra: 4 cm^{-1} for calcite (doped with selenite) and 2 cm^{-1} for pure calcite.

3.4. $Ca(OH)_2$–$CaCO_3$ transformation efficiency

Infrared spectroscopy measurements has revealed a complete $Ca(OH)_2$–calcite transformation for all calcium hydroxide carbona-

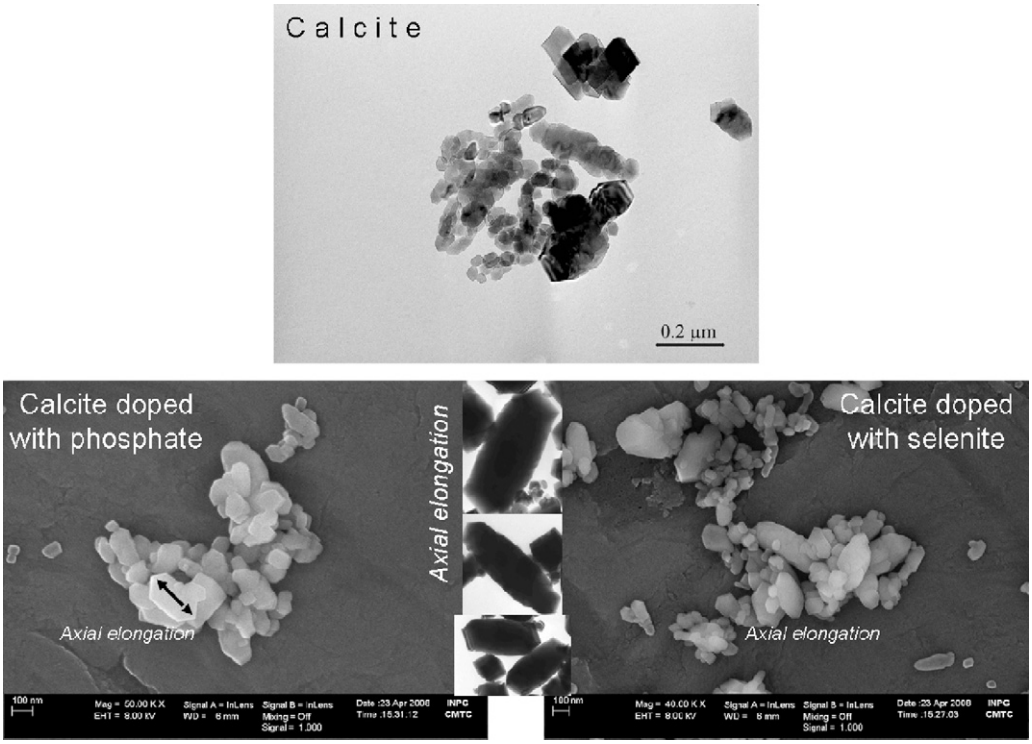

Fig. 7. TEM and SEM micrographs showing the calcite products via $Ca(OH)_2$ carbonation without or with dissolved oxyanions.

tion experiments, because the OH-stretching vibration band (ν_1) at 3642 cm^{-1} corresponding to the calcium hydroxide, was not detected in the solid product (Fig. 6a). Here, the CO_3 stretching vibration band (ν_3) at 1410–1490 cm^{-1} and the CO_3-bending vibration band (ν_2) at 877 cm^{-1} are typical fundamental bands for calcite. These results were supported by SEM and TEM observations. Concerning the oxyanion impurities (selenite, phosphate and arsenate) removed by $Ca(OH)_2$ carbonation process, only the selenite group was detected on the solid product using infrared spectrometry (Fig. 6b). The ν_1 and ν_3 SeO_3-stretching vibrations were detected at 822 and 782 cm^{-1}, respectively. Note that these values are shifted with respect to reported values for sorbed selenite onto iron oxides [40], due to solid state effects.

3.5. Crystal morphology of calcite

The TEM and SEM micrographs showed scalenohedral calcite crystals as dominant morphology. Sub-micrometric isolated particles (<0.2 μm) and micrometric aggregates and/or agglomerates (<2 μm) of calcite were observed after 3–24 h of reaction. A small proportion of rhombohedral calcite was also observed (Fig. 7). In terms of impurities effects, the selenite and phosphate produced an axial elongation of the rhombohedral calcite crystals (Fig. 7). The arsenate and non-reactive oxyanions (selenate and nitrate) had not clear effect on the crystal morphology of formed calcite. The Rietveld refinements of X-ray diffraction (XRD) spectra and N_2-adsorption measurements are envisaged in a future to quantify whether the oxyanions trapped in/on calcite produce significant effects of textural properties (specific surface area, average particle size and particle size distribution).

4. Conclusion

The main purpose of our study was to investigate the removal of oxyanions from an aqueous solution using carbonation of calcium hydroxide under moderate pressure ($P_{CO2} \cong 20$ bar) and temperature (30 °C). It was demonstrated that the $Ca(OH)_2$ carbonation allows successfully the removal of selenite (>90%), arsenate (>78%) and phosphate (≅100%) from synthetic solutions. The nitrate and selenate have not any physicochemical affinity/effect during calcite formation.

In terms of kinetic effects, it was demonstrated that the rates of CO_2 transfer during calcite formation in presence of selenite and phosphate were significantly retarded (0 < retarding factor "*RF*" < 1); a slight retarding effect was detected for arsenate ($RF \approx 0.05$) and no retarding effect was detected for selenate and nitrate ($RF \approx 0$). In general, the retarding factor for these experiments depends on the oxyanion initial concentration, oxyanion nature and $Ca(OH)_2$ dose. The presence of oxyanions could also influence the crystal morphology and aggregation/agglomeration process. For example, a *c*-axis elongation of calcite crystals was clearly observed in presence of selenite and phosphate.

The aqueous carbonation of calcium hydroxide with compressed CO_2 could be an economical and ecological method to remove various oxyanions as well as to allow the ex situ mineral sequestration of CO_2; particularly, when the $Ca(OH)_2$ source came from alkaline solid waste such as fly-ashes, waste concrete and cements, alkaline paper mill waste, etc.

Acknowledgements

The authors are grateful to the National Research Agency, ANR (GeoCarbone-CARBONATATION project), France, for providing the financial support for this work. J. Ganbaja and D. Tisserand are thanked for their technical help and assistance. Some experiments and the redaction of this study were carried out during a postdoctoral stay at the University Joseph Fourier, Grenoble ("Terre, Univers, Environnement, Société (TUNES)" post-doctoral program).

References

[1] D.M. Roundhill, H.F. Koch, Methods and technique for the selective extraction and recovery of oxoanions, Chem. Soc. Rev. 31 (2002) 60–67.

[2] T.R. Harper, N.V. Kingham, Removal of arsenic from wastewater using chemical precipitation methods, Water Environ. Res. 64 (1992) 200–203.
[3] K.R. Fox, T.J. Sorg, Controlling arsenic, fluoride and uranium by point-of-use treatment, JAWWA 79 (1987) 81–84.
[4] L.E. Eary, D. Rai, Chromate removal from aqueous waste by reduction with ferrous iron, Environ. Sci. Technol. 22 (1988) 972–977.
[5] E.H. De Carlo, D.M. Thomas, Recovery of arsenic from spent geothermal brine by flotation with colloidal ferric hydroxide and long chain alkyl surfactants, Environ. Sci. Technol. 19 (1985) 538–544.
[6] F.F. Peng, D. Pingkuan, Removal of arsenic from aqueous solution by adsorbing colloid flotation, Ind. Eng. Chem. Res. 33 (1994) 922–928.
[7] S.K. Gupta, K.Y. Chen, Arsenic removal by adsorption, J. Water Poll. Control Fend. 50 (1978) 493–506.
[8] C.P. Huang, L.K. Fu, Treatment of arsenic (V) containing water by the activated carbon process, J. Water Poll. Control Fend. 56 (1984) 233–242.
[9] Y.K. Nakano, T. Takeshita, Tsutsumi, Adsorption mechanism of hexavalent chromium by redox within condensed-tanning gel, Water Research 35 (2001) 496–500.
[10] G.M. Haggerty, R.S. Bowman, Sorption of chromate and other inorganic anions by organo zeolite, Environ. Sci. Technol. 28 (1994) 452–458.
[11] J.M. Zachara, C.E. Cowan, R.L. Schmidt, C.C. Ainworth, Chromate adsorption on amorphous iron oxyhydroxide in presence of major groundwater ions, Environ. Sci. Technol. 21 (1987) 589–594.
[12] M.M. Benjamin, Adsorption and surface precipitation of metals on amorphous iron oxyhydroxide, Environ. Sci. Technol. 17 (1983) 686–692.
[13] J.D. Peak, D.L. Sparks, Mechanisms of selenate adsorption on iron oxides and hydroxides, Environ. Sci. Technol. 36 (2002) 1460–1466.
[14] V.K. Gupta, V.K. Saini, N. Jain, Adsorption of As(III) from aqueous solutions by iron oxide-coated sand, J. Colloid Interface Sci. 288 (2005) 55–60.
[15] Derek Peak, Adsorption mechanism of selenium oxyanions at the aluminium oxide/water interface, J. Colloid Interface Sci. 303 (2006) 337–345.
[16] J.M. Ablett, C.C. Kao, R.J. Reeder, Y. Tang, A. Lanzirotti, X27A—a new hard X-ray micro-spectroscopy facility at the national synchrotron light source, Nucl. Instrum. Methods Phys. Res. 262 (2006) 487–494.
[17] G. Roman-Ross, G.J. Cuello, X. Turrillas, A. Fernandez-Martinez, L. Charlet, Arsenic sorption and co-precipitation with calcite, Chem. Geol. 233 (2006) 328–336.
[18] A. Fernandez-Martinez, G. Roman-Ross, G.J. Cuello, X. Turrillas, L. Charlet, M.R. Johnson, F. Bardelli, Arsenic uptake by gypsum and calcite: modelling and probing by neutron and X-ray scattering, Physica B 385 (2006) 935–937.
[19] V.G. Alexandratos, E.J. Elzinga, R.J. Reeder, Arsenate uptake by calcite: macroscopic and spectroscopic characterization of adsorption and incorporation mechanisms, Geochim. Cosmochim. Acta 71 (2007) 4172–4187.
[20] G. Montes-Hernandez, R. Perez-Lopez, F. Renard, J.M. Nieto, L. Charlet, sequestration of CO_2 by using carbonation of coal combustion fly-ash, J. Hazard. Mater. (2008), doi:10.1016/j.Jhazmat.2008.04.104.
[21] G. Montes-Hernandez, F. Renard, N. Geoffroy, L. Charlet, J. Pironon, Calcite precipitation from CO_2–H_2O–$Ca(OH)_2$ slurry under high pressure of CO_2, J. Crystal Growth 308 (2007) 228–236.
[22] G. Montes-Hernandez, A. Fernandez-Martinez, L. Charlet, D. Tisserand, F. Renard, Textural properties of synthetic nano-calcite produced by hydrothermal carbonation of calcium hydroxide, J. Crystal Growth 310 (2008) 2946–2953.
[23] Y.S. Han, G. Hadiko, M. Fuji, M. Takahashi, Effect of flow rate and CO_2 content on the phase and morphology of $CaCO_3$ prepared by bubbling method, J. Crystal Growth 276 (2005) 541–548.
[24] L. Moore, J.D. Hopwood, R.J. Davey, Unusual morphology and microstructures features of synthetic calcite induced by acrylate/styrene copolymers, J. Crystal Growth 261 (2004) 93–98.
[25] K.J. Westin, A.C. Rasmuson, Crystal growth aragonite and calcite in presence of citric acid, DTPA, EDTA and pyromellitic acid, J. Colloids Interface Sci. 282 (2005) 359–369.
[26] H. Tsuno, H. Kagi, T. Akagi, Effects of traces lanthanum ion on the stability of vaterite and transformation from vaterite to calcite in an aquatic system, Bull. Chem. Soc. Jpn. 74 (2001) 479.
[27] Y. Fujita, G.D. Redden, J. Ingram, M.M. Cortez, G. Ferris, R.W. Smith, Strontium incorporation into calcite generated by bacterial ureolysis, Geochim. Cosmochim. Acta 68/15 (2004) 3261–3270.
[28] S.J. Freij, A. Godelitsas, A. Putnis, Crystal growth and dissolution processes at the calcite–water interface in the presence of zinc ions, J. Crystal Growth 273 (2005) 535–545.
[29] L.A. Gower, D.A. Tirrell, Calcium carbonate films and helices grown in solutions of poly(aspartate), J. Crystal Growth 191 (1998) 153–160.
[30] R.G. Jonasson, K. Rispler, B. Wiwchar, W.D. Gunter, Effect of phosphonate inhibitors on calcite nucleation kinetics as a function of temperature using light scattering in an autoclave, Chem. Geol. 132 (1996) 215–225.
[31] A. Chrissanthopoulos, N.P. Tzanetos, A.K. Andreopoulou, J. Kallitsis, E. Dalas, Calcite crystallization on oxadiazole–tepyridine copolymer, J. Crystal Growth 280 (2005) 594–601.
[32] M. Menadakis, G. Maroulis, P.G. Koutsoukos, A quantum chemical study of doped $CaCO_3$ (calcite), Comput. Mater. Sci. 38 (2007) 522–525.
[33] E. Dousi, J. Kallitsis, A. Chrisssanthopoulos, A.H. Mangood, E. Dalas, Calcite overgrowth on carboxylated polymers, J. Crystal Growth 253 (2003) 496–503.
[34] L. Pastero, E. Costa, B. Alessandria, M. Rubbo, D. Aquilano, The competition between {1014} cleavage and {0112} steep rhombohedra in gel grown calcite crystal, J. Crystal Growth 247 (2003) 472–482.
[35] Y.J. Lee, R. Reeder, The role of citrate and phthalate during Co(II) coprecipitation with calcite, Geochem. Cosmochem. Acta 70 (2006) 2253–2269.
[36] M. Temmam, J. Paquette, H. Vali, Mn and Zn incorporation into calcite as a function of chloride aqueous concentration, Geochem. Cosmochem. Acta 64 (2000) 2417–2430.
[37] E. Dalas, A. Chalias, D. Gatos, K. Barlos, The inhibition of calcium carbonate crystal growth by the cysteine-rich Mdm2 petide, J. Colloids Interface Sci. 300 (2006) 536–542.
[38] R. Perez-Lopez, G. Montes-Hernandez, J.M. Nieto, F. Renard, L. Charlet, Carbonation of alkaline paper mill waste to reduce CO_2 greenhouse gas emissions into the atmosphere, Appl. Geochem. (2008), doi:10.1016/j.apgeochem.2008.04.016.
[39] G. Montes-Hernandez, S. Rihs, A simplified method to estimate kinetic and thermodynamic parameters on the solid–liquid separation of pollutants, J. Colloids Interface Sci. 299 (2006) 49–55.
[40] C. Su, D.L. Suarez, Selenate and selenite sorption on iron oxides: an infrared and electrophoretic study, Soil Sci. Soc. Am. J. 64 (2000) 101–111.